

# High-Range Resolution Radar for the Identification of Approaching Targets : Effects of Parameters and Measurements

*Christian Bouchard, étudiant 2<sup>e</sup> cycle*

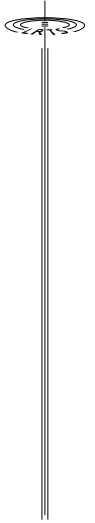
*Dr Dominic Grenier, directeur de recherche*

*Abstract: With radar signals without compression, the resolution is fixed by the pulses' lengths. For short targets, the scatterers are closely spaced and their echoes overlap making them indistinguishable. To overcome this, an algorithm based on the MUSIC algorithm was developed and simulations have shown the improvement on the radar's range resolution. In the present work, we have carried on with the simulations to estimate the effects of the most important parameters needed by the algorithm and we have made measurements to demonstrate the possible use of the method in the real world.*

*Résumé: Lorsqu'on utilise des signaux radar sans compression, la résolution est fixée par la durée des impulsions. Pour de courtes cibles, les points réflecteurs sont près les uns des autres et leurs échos se superposent ce qui les rend indissociables. Pour contrer ce problème, un algorithme basé sur l'algorithme MUSIC a été développé et des simulations ont démontré l'amélioration de la résolution en portée du radar. Dans le présent travail, les simulations ont été poursuivies, dans le but d'estimer l'effet des plus importants paramètres sur la résolution, et des mesures ont été effectuées pour démontrer l'utilisation possible de la méthode.*

## **Introduction**

For the identification of targets coming face to the radar by a radar signature, a very high-range resolution is required to resolve the target into its principal scatterers and to obtain an estimate of the target length in the range direction. When the distance between the scatterers becomes smaller than the radar's resolution, the echoes overlap and it is impossible to measure the delay between the echoes. To solve this problem, the HRR-HRM algorithm uses a subsampling of the short RF pulses to estimate the covariance matrix of the received signal and it takes into account the movement of the target toward the radar during the sampling. The covariance matrix is later processed with a time adaptation of the MUSIC algorithm allowing a higher resolution than with classical signal processing methods such as envelope correlation, FFT, etc.



In this paper, we will discuss the different RF signals and the subsampling method, the time adaptation of the MUSIC algorithm and finally the effects of the most important parameters using simulations and measurements.

## RF signals and subsampling method

The HRR-HRM algorithm uses, up to now, two types of modulation of the radar pulses : AM with very short pulses as modulating signal and stepped-frequency from pulse to pulse. With the time adaptation of MUSIC, the resolution is linked to the time between the samples. As this time cannot be made as short as we would want due to the current technology and power limitation, we use a subsampling technique.

With AM modulation, the same carrier  $f_0$  is used for all pulses which repeat themselves every  $1/PRF$  seconds, where  $PRF$  is the pulse repetition frequency. The subsampling recovers a spread pulse every  $N/PRF$  seconds approximately.  $N$  is the number of pulses used by the subsampling to form one snapshot. The subsampling method is shown in Figure 1(a) where  $T_s$  is the sampling periode,  $\tau_s$  the subsampling step and  $\Delta T$  the reduction of time between the pulses caused by the movement of the target toward the radar.

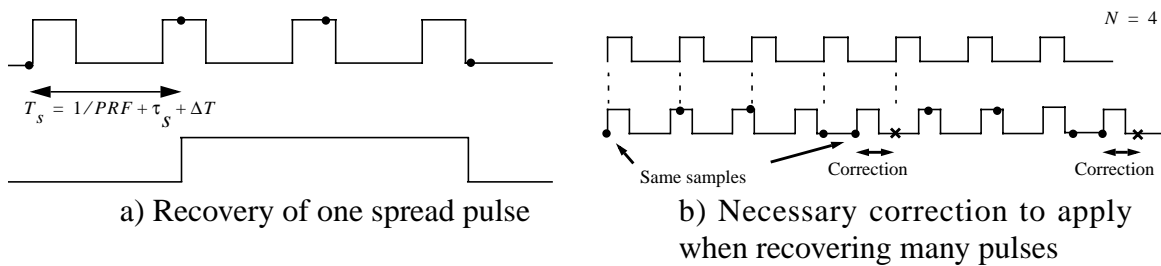


**Figure 1** Subsampling of the received signal

This target motion causes the time between the received pulses to diminish, which leads to two effects that must be taken into account. First, we must correct the moment at which we start the subsampling (Figure 1(b)). The decrease of time between two pulses equals  $\Delta T = 2v/PRFc$ . We use  $N$  pulses to recover one, so we must start the new subsampling  $2Nv/PRFc$  seconds before the moment we would do it if the target were stationary. Second, as the total subsampling step is higher than  $\tau_s$  by an amount  $\Delta T$ , the target seems shorter, so we must apply a rescaling factor to the result, before displaying the image, which was not done prior to this work. The subsampling spreads the pulses in time, so the total rescaling factor is now :

$$\tau_{\text{real}} = \tau_{\text{spread}} \left[ \frac{\tau_s PRF + \frac{2v}{c}}{1 + \tau_s PRF + \frac{2v}{c}} \right] \quad (1)$$

The previous discussion is also valid for the stepped-frequency modulation, except that we use  $K$  different carriers. We use a carrier  $f_0$  for all pulses of the first snapshot which recovers a spread pulse. The second snapshot is done with a carrier  $f_1$ , and so on, until the  $k^{\text{th}}$  snapshot which will be done with the carrier  $f_0$  and will initiate another cycle.

To realize the subsampling and the rescaling shown in (1), we must know *a priori* the target speed and range which are obtainable as part of the detection process.

### Time adaptation of the MUSIC algorithm

The HRR-HRM uses a time adaptation of the MUSIC algorithm [1], [2]. The present development follows closely [3][3].

To use the adaptation, we have to estimate the covariance matrix of the received signal. To do this, we realize  $L$  snapshots with the subsampling technique described earlier. We have  $L$  snapshots of  $N$  samples each, allowing us to estimate the expected value of the sampled signal.

The received signal can be written as

$$r(t) = \sum_{i=1}^M \alpha_i s(t - \tau_i) + n_0(t) \quad (2)$$

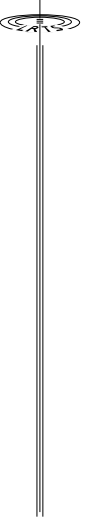
where  $M$  is the number of scatterers and  $\alpha_i = |\alpha_i| e^{j\phi_i}$ . The amplitudes  $|\alpha_i|$  are rayleigh distributed and the phases  $\phi_i$  are uniformly distributed. The complex exponentials of different frequencies of MUSIC are replaced by a complex signal  $s(t)$  with  $M$  different time delays which correspond to the different scatterers.

The  $l^{\text{th}}$  snapshot can be written as  $\mathbf{r} = \mathbf{S}\mathbf{a} + \mathbf{n}$  where :

$$\mathbf{S} = \begin{bmatrix} s(t_1 - \tau_1) & s(t_1 - \tau_2) & \dots & s(t_1 - \tau_M) \\ s(t_2 - \tau_1) & s(t_2 - \tau_2) & \dots & s(t_2 - \tau_M) \\ s(t_3 - \tau_1) & \dots & \dots & s(t_3 - \tau_M) \\ \dots & \dots & \dots & \dots \\ s(t_N - \tau_1) & \dots & \dots & s(t_N - \tau_M) \end{bmatrix} \quad (3)$$

$$\mathbf{a} = [\alpha_1 \ \alpha_2 \ \dots \ \alpha_M]^T \quad (4)$$

$$\mathbf{n} = [n(t_1) \ n(t_2) \ \dots \ n(t_M)]^T \quad (5)$$



The covariance matrix is built as follow :

$$\mathbf{R} = \frac{1}{L} \begin{bmatrix} \sum_{i=1}^L r_i(t_1) r_i^*(t_1) & \dots & \sum_{i=1}^L r_i(t_1) r_i^*(t_N) \\ \dots & \dots & \dots \\ \sum_{i=1}^L r_i(t_N) r_i^*(t_1) & \dots & \sum_{i=1}^L r_i(t_N) r_i^*(t_N) \end{bmatrix}. \quad (6)$$

We find the eigenvectors  $\mathbf{v}_i$  and eigenvalues  $\lambda_i$  of the matrix  $\mathbf{R}$  and form the signal and noise subspaces. The number of scatterers,  $M$ , can be estimated by looking at the highest eigenvalues with the help of a method such as the Akaike information criterion (AIC).

Now that we know which vectors form the signal subspace and which ones form the noise subspace, we can form the function

$$\Phi(\tau) = \frac{\sum_{i=1}^M |s^*(\tau) \mathbf{v}_i|^2}{\sum_{j=M+1}^N |s^*(\tau) \mathbf{v}_j|^2}. \quad (7)$$

The function  $\Phi(\tau)$  will show, in theory, maximums for values of  $\tau$  that represent delays in the received signal which correspond to scatterers. By applying the rescaling factor (1) multiplied by  $c/2$  to  $\tau$  in (7), we obtain the target image in the range direction with the right space-delay dimension.

## Simulation results

A series of simulations were done to evaluate the effects of the most important parameters on the estimation of the target's length. The targets are made of two scatterers, one at the front and one at the back. The HRR-HRM algorithm gives the image in range and the distance between the two scatterers. We modify the distance between the scatterers to observe the length estimated by the algorithm for targets of different lengths. The parameters fixed for all the simulations are :  $f_0 = 10$  GHz,  $PRF = 10$  kHz and the target begins its course at 10 km from the radar. On some graphics, the length of the simulated targets is represented on the horizontal axis and the relative error is on the vertical axis. A positive error means that the algorithm overestimates the target's length while a negative error means an underestimation. On other graphics, we show the time-domain pseudospectrum which corresponds to the target image in the range direction. Our definition of the signal-to-noise ratio (SNR) is the power ratio between one scatterer's strength and the noise's variance at each sensor. We compare the resolution obtained with the algorithm to the resolution limit obtained when no high-resolution processing is used given by the Rayleigh criterion defined as  $\Delta R = T_{\text{pulse}} c/2$ .

### Signal-to-noise ratio

As we might expect, the SNR has a very important effect on the results. With the AM modulation, for a SNR higher or equal to -3 dB the results are similar (Figure 2(a), where the pulses have 16 ns, the target speed is 100 m/s and well evaluated as it is the case when not specified). The results are good for lengths higher than 0.3 m and the uncertainty on the target length is  $\Delta L = \tau_y c/2 = 0.15$  m. Without processing, the Rayleigh criterion is 2.4 m.

When the SNR is diminished under -3 dB, the results deteriorate and become unstable under -6 dB (Figure 2(b)). The results with the stepped-frequency modulation are very similar to those obtained with the AM modulation. However, by looking at the target's image for different modulations (Figure 3), we observe that the amplitude of the pseudo-spectrum is lower for the stepped-frequency modulation, resulting in a more difficult estimation of the target's length. For this reason, the rest of this paper will only discuss HRR-HRM with the AM modulation.

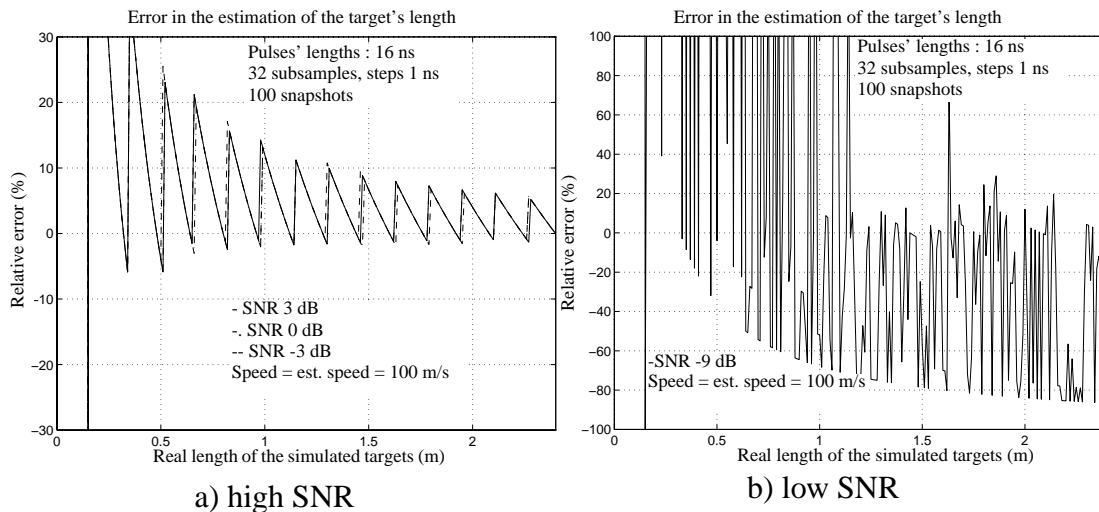


**Figure 2** Effects of the SNR on the evaluation of the target's length

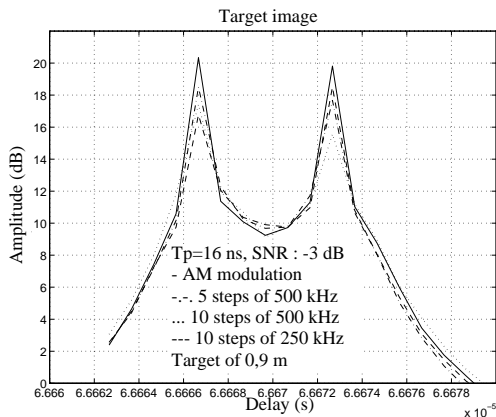


**Figure 3** Target image : different modulations

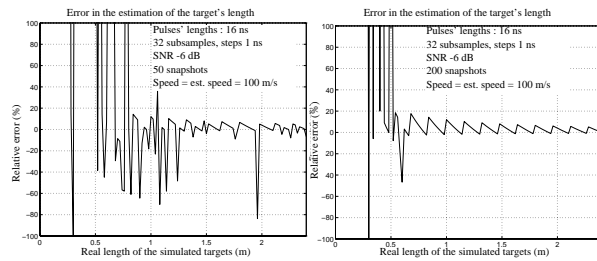


**Figure 4** Effects of the number of snapshots at low SNR

### Number of snapshots

To evaluate the covariance matrix, we realize a number of snapshots with the subsampling method discussed earlier. At strong SNR, the results are the same no matter how many snapshots are used. The results are similar to those shown in Figure 2(a). While for SNR lower than -3 dB, the results improve as the number of snapshots is raised (Figure 4). This is explained by the integration which gives a better estimation of the covariance matrix. Theoretically, doubling the number of snapshots would be equivalent to raise the SNR by 3 dB.

The subsampling step also has an important effect on the resolution. Figure 5 shows that, as the subsampling step is lowered, the precision on the evaluation of the target's length becomes better and it is also possible to observe shorter targets. It is important to take into account the contribution of the target speed to the subsampling step. For example, with a speed of 350 m/s,  $\Delta T = 0.233$  ns, if the subsampling step is 0.5 ns then the contribution of  $\Delta T$  is 45% of the total subsampling step.

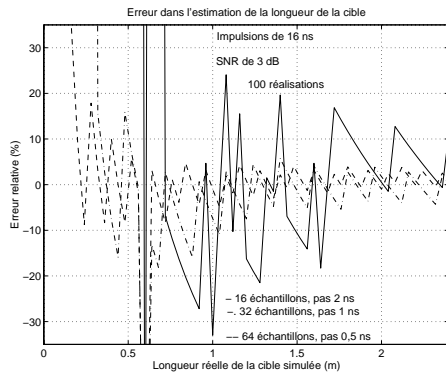


**Figure 5** Effects of the subsampling step

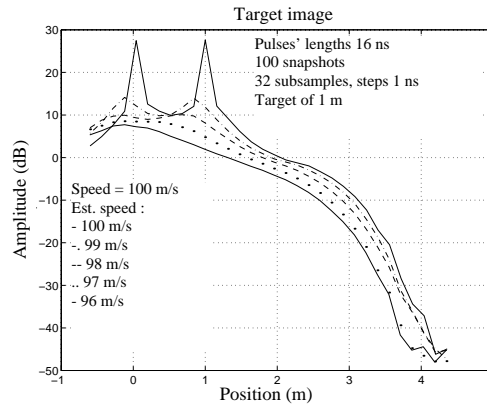


**Figure 6** Target Image : error in the estimation of the target speed

### Error in the estimation of the target speed

An error in the estimation of the target speed causes a diminution of the peaks' amplitude in the time-domain pseudospectrum. On Figure 6, we see that when errors over 3 m/s are made in the estimation of the target speed, the amplitude has vanished enough that we cannot see at all the two scatterers. A final explanation why this occurs for such low errors has not been found yet but this is due in part to the error accumulation on the time at which the sampling is done. A solution would be to evaluate the target speed while the data are taken.

## Experimental results

To do the experiments, we have used the small radar made by Lab-Volt which already uses a subsampling (1024 pulses at a  $PRF = 295$  kHz to recover one pulse) so we did not use the subsampling method described earlier. The carrier frequency is 9,4 GHz. The pulses have 5 ns which, without any processing, would give a resolution of 0.75 m. Figure 7 shows a exemple of experimental result where we see two peaks for the two scatterers. The estimated length is slightly lower than the real length.

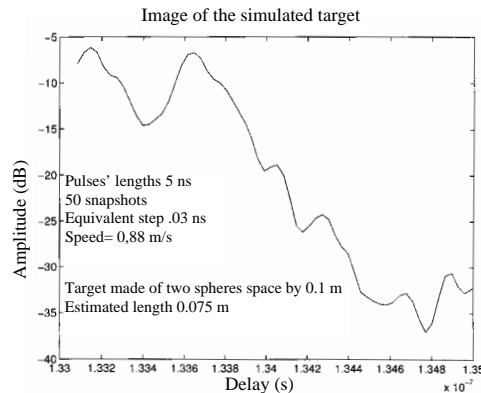
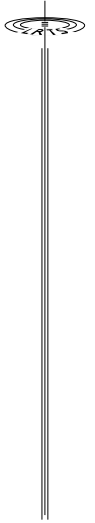


Figure 7 Target image : measurement

## Conclusion

The effects of the parameters on the results given by the HRR-HRM algorithm have been evaluated. A SNR of at least -3 dB and a very good evaluation of the target speed have been shown to be necessary to obtain good results. Measurements have demonstrated the possible use of the HRR-HRM algorithm in the real world.

## Acknowledgements

This work was done as part of a contract with the Department of National Defence. Éric Pigeon has developed the algorithm and has done the initial testing. Éric Bellavance has added the stepped-frequency modulation and has realized the experiments in collaboration with Jean-René Larocque.

## References

- [1] R. O. Schmidt, "Multiple emitter location and signal parameter estimation", in *Proc. RADC Spectrum Estimat. Workshop*, Oct. 1979.
- [2] C. W. Therrien, *Discrete Random Signals and Statistical Signal Processing*. Englewood Cliffs, NJ: Prentice-Hall, 1992
- [3] D. Grenier, É. Pigeon and R. M. Turner, "High-range resolution mono-frequency pulsed radar for the identification of approaching targets using subsampling and the MUSIC algorithm", *IEEE signal processing letters*, vol. 3 no. 6 june 1996.